Cascade First and Second Order Sliding Mode Controller of a QuadRotor UAV based on Exponential Reaching Law and Modified Super-Twisting Algorithm

E. Paiva[1], M. Gomez-Redondo[1], J. Rodas[1], Y. Kali[2], M. Saad[2], R. Gregor[1], H. Fretes[1]

***Abstract*— Unmanned aerial vehicles have become a disruptive technology, which has experienced exponential growth in several applications. The control of these vehicles is a fairly wide area and the cascade PID controller is the most used in practice. However, this latter structure doesn't ensure high performances in the presence of unmodelled dynamics, uncertainties and external abrupt disturbances. To that end, this work proposes a new method that consists of a non-linear cascade configuration of the variable structure control between first order sliding mode based on exponential reaching law and modified super-twisting second order sliding mode algorithm. The developed method is tested on simulation on a quadrotor system, the results obtained demonstrate good performance for trajectory tracking and as well as other non-linear controller options, it is robust against unmodeled dynamics and disturbances.**

I. Introduction

Unmanned Aerial Vehicles (UAV) are systems present in multiple applications related to agriculture such as control and prevention of plant diseases, weeds identification, insect pests and production estimates [1], photogrammetry since UAVs allow fast, accurate and economical scanning of a surface compared to terrestrial, satellite and manned aerial methods [2], inspections of power lines replacing traditional methods such as helicopters or cars, which are often expensive, slow and potentially dangerous [3], load transporting system for environments where geographical conditions are unfavourable [4], [5], security such as remote traffic monitoring and frontier patrols [6], and others [7]. These applications are developed in different operating environments, with a variety of disturbances such as wind and uncertainties that can cause instability.

Currently, there are multiple control algorithms that allow the tracking and stabilization of UAVs, linear controllers such as PID, pole placement or LQR [8] are powerful methods to control systems, but if operating conditions modify the dynamics of the system, the gains of each controller must be changed for stabilization. non-linear control systems are controllers that use the mathematical model of the system studied, within the classification of the controllers are feedback linearization, backstepping, fuzzy logic controllers and sliding mode.

Sliding Mode (SM) is a famous robust nonlinear techniques and well-known for its effectiveness and powerful properties that attract the community of automation researcher [9]. Indeed, the three good features of SM controller are: robustness against a large class of uncertainties, development's simplicity and finite-time convergence. This method uses discontinuous input signals that switch highly to force the system's states to converge in finite-time to the so-called switching function and then to move throughout this surface towards the equilibrium point. SM controller has been tested in simulation and in real time on different nonlinear systems such as electric drive machines [10], [11], highly coupled robot systems [12], [13] and underactuated nonlinear systems as UAVs [14]. Nevertheless, its real-time application still restricted because of the problem of the chattering phenomenon [15]. This problem is considered as the major disadvantage of SM controller since it can lead to very bad performances and the wear of the system's mechanical parts.

In literature, many researchers tried to solve this problem [16]–[19]. The most attractive proposed solution consists of an augmented SM that is known under the name Second Order Sliding Mode (SOSM) [20]. Unlike the classical SM, the SOSM control signals that fed into the system are continuous [21], [22] since the the switching signals act on the derivative of the control inputs. However, its real-time implementation still limited due to the lack of required informations (measurement of the first time derivative of the selected switching function). This problem has been solved by the proposition of the Super-Twisting Algorithm (STA) [23]–[27].

In this paper, considering a quadrotor UAV that is a non-linear underactuated system because its number of degrees of freedom is greater than the number of independent control inputs. The contribution of this work focuses on the proposed sliding mode controller in cascade [28], with an outer position control loop based on the exponential reaching law (ERL) and an inner Attitude/Altitude control loop based on Modified Super-Twisting Algorithm (Modified STA). This cascade configuration is commonly seen in practice with PIDs for pixhawk-based UAV control. The original contribution is to make the inner control loop faster than the outer control loop while ensuring robustness against

[1]Enrique Paiva, Marcos Gomez-Redondo, Jorge Rodas, Raul Gregor and Hector Fretes are with the Laboratory of Power and Control Systems, Facultad de Ingeniería, Universidad Nacional de Asunción, Luque, Paraguay. (enpaiva93@gmail.com, gomezredondomarcos@gmail.com, jrodas@ing.una.py, rgregor@ing.una.py)

[2]Yassine Kali and Maarouf Saad are with the Department of Electrical Engineering, École de Technologie Supérieure, Montreal, QC H3C 1K3, Canada. (y.kali88@gmail.com, maarouf.saad@etsmtl.ca)

uncertainties, unmodelled dynamics and perturbations.

The present paper is divided into six sections as follows. In the following section, the full position and attitude mathematical models of the quadrotor UAV system. In Section IV, the simplify position and attitude mathematical models to use in the controller. In Section V the sliding mode controller. In Section VI, numerical simulations of the UAV studied to show the performance of the proposed controller in the presence of perturbation and unknown dynamics. The conclusion is in the last section.

II. Mathematical Model

The system consists of a UAV quadrotor (Fig. 1). The complete mathematical model of the position and attitude is detailed in (1) and (2), respectively [29].

$$\ddot{P} = \left(\frac{R^T}{\mathrm{m}}\right)\left(F - \mathrm{m}\,\dot{R}\,\dot{P} - \mathrm{m}\left(W\,\dot{\Theta}\times R\,\dot{P}\right)\right) \tag{1}$$

$$F = \begin{bmatrix} 0 \\ 0 \\ \tau_1 \end{bmatrix} + \mathrm{m}\,\mathrm{g}\,R\begin{bmatrix} 0 \\ 0 \\ 1 \end{bmatrix}$$

$$\ddot{\Theta} = (J\,W)^{-1}\left(\tau - \left(W\,\dot{\Theta}\times J\,W\,\dot{\Theta}\right) - J\,\dot{W}\,\dot{\Theta}\right) \tag{2}$$

where $P = [X, Y, Z]^T$ represents the vector inertial position of an UAV (North, East and Down), $\Theta = [\phi, \theta, \psi]^T$ represents the vector of Euler angles, g is the gravity constant, m denotes the mass of the vehicule, $J = \mathrm{diag}(J_x, J_y, J_z)$ represents the inertia matrix, τ_1 is the sum of the vertical forces generated by each propeller, $\tau = [\tau_\phi, \tau_\theta, \tau_\psi]^T$ denotes the torque vector with its roll, pitch and yaw components.

On the other hand, $W \in \mathcal{R}^{3\times3}$ denotes the matrix of Euler defined by:

$$W = \begin{bmatrix} 1 & 0 & -s_\theta \\ 0 & c_\phi & c_\theta\, s_\phi \\ 0 & -s_\phi & c_\theta\, c_\phi \end{bmatrix}.$$

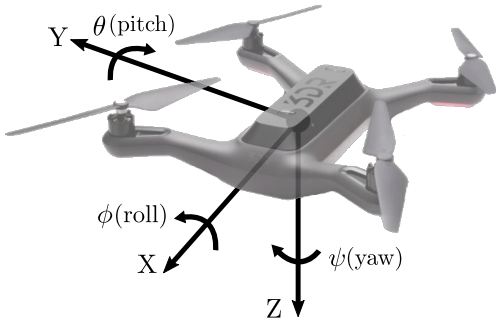

Fig. 1. Quadrotor UAV.

and $R \in \mathcal{R}^{3\times3}$ denotes the matrix transformation to the body frame given by:

$$R^T = \begin{bmatrix} c_\theta c_\psi & s_\phi s_\theta c_\psi - c_\phi s_\psi & c_\phi s_\theta c_\psi + s_\phi s_\psi \\ c_\theta s_\psi & s_\phi s_\theta s_\psi + c_\phi c_\psi & c_\phi s_\theta s_\psi - s_\phi c_\psi \\ -s_\theta & s_\phi c_\theta & c_\phi c_\theta \end{bmatrix}$$

with $c_x = \cos(x)$ and $s_x = \sin(x)$.

The control torque inputs are:

$$\begin{bmatrix} \tau_1 \\ \tau_\phi \\ \tau_\theta \\ \tau_\psi \end{bmatrix} = \underbrace{\begin{bmatrix} -1 & -1 & -1 & -1 \\ l_2 & -l_2 & -l_2 & l_2 \\ l_1 & l_1 & -l_1 & -l_1 \\ -1 & 1 & -1 & 1 \end{bmatrix}}_{\mathrm{T}} \begin{bmatrix} f_1 \\ f_2 \\ f_3 \\ f_4 \end{bmatrix} \tag{3}$$

where f_1, f_2, f_3 and f_4 represent the thrust produced by the four rotors, l_1 and l_2 are the lengths shown in Fig. 2.

In addtion, each force is computed using the inverse of the above matrix equality as:

$$\begin{bmatrix} f_1 \\ f_2 \\ f_3 \\ f_4 \end{bmatrix} = T^{-1}\begin{bmatrix} \tau_1 \\ \tau_\phi \\ \tau_\theta \\ \tau_\psi \end{bmatrix}. \tag{4}$$

III. Mathematical Model for Controller

Since (1) and (2) are complex representations and difficult to implement in-flight controllers, a simplified representation of them was obtained as shown below:

$$\ddot{X} = \frac{\tau_1}{\mathrm{m}}\left(\sin(\phi)\sin(\psi) + \cos(\phi)\sin(\theta)\cos(\psi)\right) \tag{5}$$

$$\ddot{Y} = \frac{\tau_1}{\mathrm{m}}\left(\cos(\phi)\sin(\theta)\sin(\psi) - \sin(\phi)\cos(\psi)\right) \tag{6}$$

$$\ddot{Z} = \frac{\tau_1}{\mathrm{m}}\left(\cos(\phi)\cos(\theta)\right) + \mathrm{g} \tag{7}$$

$$\ddot{\phi} = \frac{\tau_\phi}{J_x} + \frac{\tau_\theta}{J_y}\sin(\phi)\tan(\theta) + \frac{\tau_\psi}{J_z}\cos(\phi)\tan(\theta) \tag{8}$$

$$\ddot{\theta} = \frac{\tau_\theta}{J_y}\cos(\phi) - \frac{\tau_\psi}{J_z}\sin(\phi) \tag{9}$$

$$\ddot{\psi} = \frac{\tau_\theta}{J_y}\sin(\phi)\sec(\theta) + \frac{\tau_\psi}{J_z}\cos(\phi)\sec(\theta). \tag{10}$$

This set of equations are regrouped as follows:

$$\begin{aligned} \dot{\chi}_1 &= \chi_2, \\ \dot{\chi}_2 &= \mathrm{F}(\chi) + \mathrm{G}(\chi)\,u + h. \end{aligned} \tag{11}$$

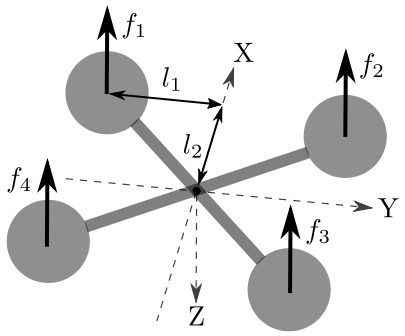

Fig. 2. Force diagram of the Quadrotor UAV.

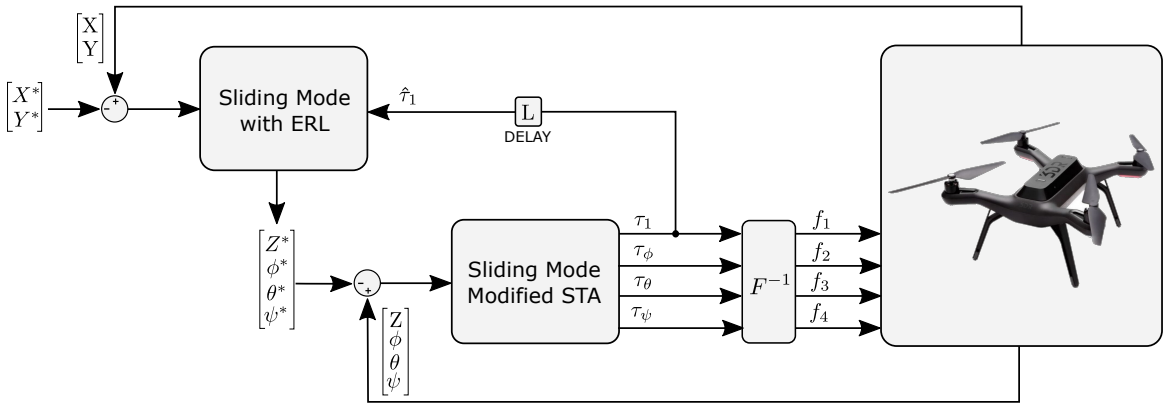

Fig. 3. Block diagram of the closed-loop quadrotor UAV.

where $\chi_1 = [X, Y, Z, \phi, \theta, \psi]^T$ is the state variables vector with and $h \in \mathcal{R}^6$ represents the uncertain vector with unmodeled dynamics and/or perturbations. Based on (5)-(10), the following equivalences are given:

$$\mathrm{F}(\chi) = \begin{bmatrix} 0 & 0 & \mathrm{g} & 0 & 0 & 0 \end{bmatrix}^T$$

$$\mathrm{G}(\chi) = \begin{bmatrix} g_{11} & g_{12} & 0 & 0 & 0 & 0 \\ g_{21} & g_{22} & 0 & 0 & 0 & 0 \\ 0 & 0 & g_{33} & 0 & 0 & 0 \\ 0 & 0 & 0 & g_{44} & g_{45} & g_{46} \\ 0 & 0 & 0 & 0 & g_{55} & g_{56} \\ 0 & 0 & 0 & 0 & g_{65} & g_{66} \end{bmatrix}$$

$$g_{11} = \frac{\hat{\tau}_1 \cos(\psi)}{\mathrm{m}} \qquad g_{12} = \frac{\hat{\tau}_1 \sin(\psi)}{\mathrm{m}}$$
$$g_{21} = \frac{\hat{\tau}_1 \sin(\psi)}{\mathrm{m}} \qquad g_{22} = -\frac{\hat{\tau}_1 \cos(\psi)}{\mathrm{m}}$$
$$g_{33} = \frac{\cos(\phi)\cos(\theta)}{\mathrm{m}} \qquad g_{44} = \frac{1}{J_x}$$
$$g_{45} = \frac{\sin(\phi)\tan(\theta)}{J_y} \qquad g_{46} = \frac{\cos(\phi)\tan(\theta)}{J_z}$$
$$g_{55} = \frac{\cos(\phi)}{J_y} \qquad g_{56} = -\frac{\sin(\theta)}{J_z}$$
$$g_{65} = \frac{\sin(\phi)\sec(\theta)}{J_y} \qquad g_{66} = \frac{\cos(\phi)\sec(\theta)}{J_z}$$

$$u = [u_1, u_2]^T$$
$$u_1 = [\cos(\phi)\sin(\theta),\ \sin(\phi)]$$
$$u_2 = [\tau_1,\ \tau_\phi,\ \tau_\theta,\ \tau_\psi]\,.$$

In the control matrix $\mathrm{G}_1(\chi)$, $\hat{\tau}_1$ represents the following delayed vertical force:

$$\hat{\tau}_1(t) = \tau_1(t - L),$$

where L is the time delay which is often selected to be the sampling time.

IV. Sliding Mode Controller

The proposed method consists of a cascade sliding mode based on a Proportional-Derivative sliding surface. The inner control loop uses Modified STA to control of attitude and altitude of UAV, whereas the outer control loop uses SM controller with ERL in the UAV position controller and generates the reference signals for the inner control loop Fig. 3. The developed controller will ensure the convergence of the system's state χ_1 to the desired trajectory vector $\chi_1^* = [X^*, Y^*, Z^*, \phi^*, \theta^*, \psi^*]^T$ with ϕ^* and θ^* are computed as:

$$\begin{bmatrix} \phi^* \\ \theta^* \end{bmatrix} = \sin^{-1}\left(\begin{bmatrix} u_2 \\ u_1/\cos(\sin^{-1}(u_2)) \end{bmatrix}\right).$$

The trajectory tracking error is represented by $e = \chi_1 - \chi_1^*$ and the sliding surface selected in this paper is:

$$S = \dot{e} + K_p\, e \tag{12}$$

where $K_p = \mathrm{diag}(K_{p1}, K_{p2}, \cdots, K_{p6})$ is a diagonal positive definite matrix. Now, let us use (11) to compute the time derivative of the selected linear switching function S as follows:

$$\begin{aligned} \dot{S} &= \ddot{e} + K_p\, \dot{e} \\ &= \dot{\chi}_2 - \ddot{\chi}_1^* + K_p\, \dot{e} \\ &= \mathrm{F}(\chi) + \mathrm{G}(\chi)\, u - \ddot{\chi}_1^* + K_p\, \dot{e}. \end{aligned} \tag{13}$$

The vector of cascade sliding mode controller, combined sliding mode with ERL [30] and Modified STA [28] is:

$$\dot{S} = \begin{bmatrix} -\dfrac{K_{11}}{N(S_1)}\,\mathrm{sign}(S_1) - K_{12}\, S_1 + \dot{\varpi}_1 \\ -\dfrac{K_{21}}{N(S_2)}\,\mathrm{sign}(S_2) - K_{22}\, S_2 + \dot{\varpi}_2 \\ -K_{31}\,|S_3|^{0.5}\,\mathrm{sign}(S_3) - K_{32}\, S_3 + \dot{\varpi}_3 \\ -K_{41}\,|S_4|^{0.5}\,\mathrm{sign}(S_4) - K_{42}\, S_4 + \dot{\varpi}_4 \\ -K_{51}\,|S_5|^{0.5}\,\mathrm{sign}(S_5) - K_{52}\, S_5 + \dot{\varpi}_5 \\ -K_{61}\,|S_6|^{0.5}\,\mathrm{sign}(S_6) - K_{62}\, S_6 + \dot{\varpi}_6 \end{bmatrix} \tag{14}$$

where $N(S_i) = \delta_0 + (1 - \delta_0)\,\mathrm{e}^{-a\,|S_i|^p}$ for $i = 1, 2$ with $0 < \delta_0 < 1$ and $a, p > 0$ [31].

$$\dot{\varpi} = \begin{bmatrix} 0 \\ 0 \\ -K_{33}\,\mathrm{sign}(S_3) - K_{34}\,\varpi_3 \\ -K_{43}\,\mathrm{sign}(S_4) - K_{44}\,\varpi_4 \\ -K_{53}\,\mathrm{sign}(S_5) - K_{54}\,\varpi_5 \\ -K_{63}\,\mathrm{sign}(S_6) - K_{64}\,\varpi_6 \end{bmatrix} \tag{15}$$

with the sign function:

$$\text{sign}(S_i) = \begin{cases} 1, & \text{if } S_i > 0, \\ 0, & \text{if } S_i = 0, \\ -1, & \text{if } S_i < 0. \end{cases} \tag{16}$$

Hence, combining (13) and (14) gives the following control law expression:

$$\begin{aligned} u =& \mathrm{G}^{-1}(\chi)\left(\ddot{\chi}_1^* - K_p\,\dot{e} - \mathrm{F}(\chi)\right) \\ &+ \mathrm{G}^{-1}(\chi)\begin{bmatrix} -\dfrac{K_{11}}{N(S_1)}\,\text{sign}(S_1) - K_{12}\,S_1 + \dot{\varpi}_1 \\ -\dfrac{K_{21}}{N(S_2)}\,\text{sign}(S_2) - K_{22}\,S_2 + \dot{\varpi}_2 \\ -K_{31}\,|S_3|^{0.5}\,\text{sign}(S_3) - K_{32}\,S_3 + \dot{\varpi}_3 \\ -K_{41}\,|S_4|^{0.5}\,\text{sign}(S_4) - K_{42}\,S_4 + \dot{\varpi}_4 \\ -K_{51}\,|S_5|^{0.5}\,\text{sign}(S_5) - K_{52}\,S_5 + \dot{\varpi}_5 \\ -K_{61}\,|S_6|^{0.5}\,\text{sign}(S_6) - K_{62}\,S_6 + \dot{\varpi}_6 \end{bmatrix} \end{aligned} \tag{17}$$

The detailed stability analysis can be found in [28], [32].

V. Simulation Results

In this section, Matlab/Simulink is the software used to simulate the performance of the cascade sliding mode controller. The simplified mathematical model allows simulating conditions of unmodeled dynamics and we added Gaussian noise on each state variable (Fig. 4).

The physical parameters are shown in the Table I.

TABLE I

Quadrotor UAV's parameters.

Parameters	Value
Mass, m	4 Kg
Moment of inertia, J_x	0.111132 Kg.m^2
Moment of inertia, J_y	0.13282 Kg.m^2
Moment of inertia, J_z	0.249039 Kg.m^2
Length, l_1	0.2 m
Length, l_2	0.2 m
Gravity, g	9.81 m.s^{-2}

The gains for sliding surface are K_p=diag$(1, 1, 1, 5, 5, 5)$ and for cascade sliding mode controller are in Table II. All these gains were found heuristically.

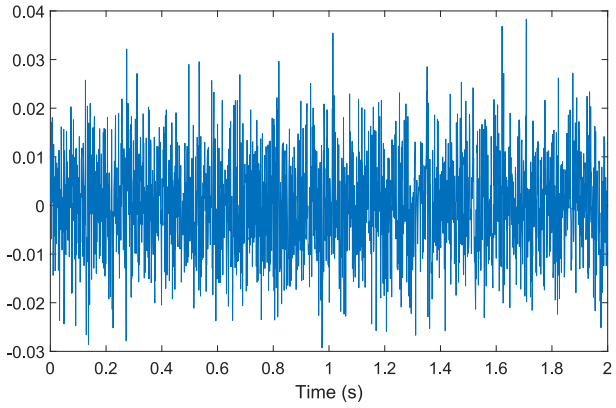

Fig. 4. Disturbances on each position and each Euler Angle of UAV.

The time delay between outer/inner controls loop is $L = 0.006$ s, while the sampling time for outer loop control is 10^{-2} s and for the inner control loop is 0.004 s.

TABLE II

Sliding Mode controller gains.

Gains	Values	Gains	Values	Gains	Values
K_{11}	0.1	K_{41}	1.5	K_{61}	1
K_{12}	0.5	K_{42}	7.5	K_{62}	5
K_{21}	0.1	K_{43}	7.5	K_{63}	5
K_{22}	0.5	K_{44}	7.5	K_{64}	5
K_{31}	2	K_{51}	0.1	δ_0	0.1
K_{32}	2	K_{52}	1	p	3
K_{33}	2	K_{53}	1	a	2
K_{34}	2	K_{54}	1		

The simulation consists of tracking a square path with different values of orientation angles (ψ). The tracking results are in Fig. 5 and Fig. 6, along with the desired paths. The Fig. 7 corresponds to the thrusts for the UAV generated by the controller and the three-dimensional path is shown in Fig. 8.

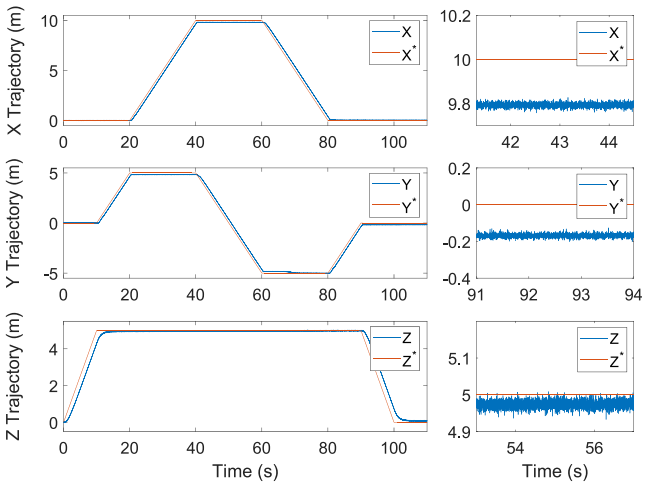

Fig. 5. Simulation results of position tracking.

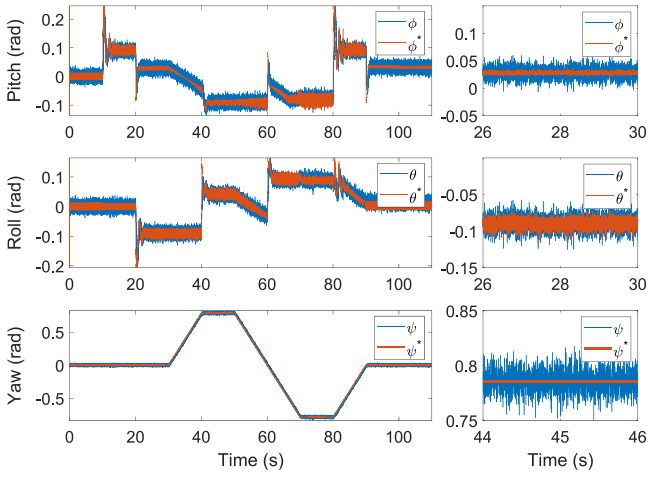

Fig. 6. Simulation results of attitude tracking.

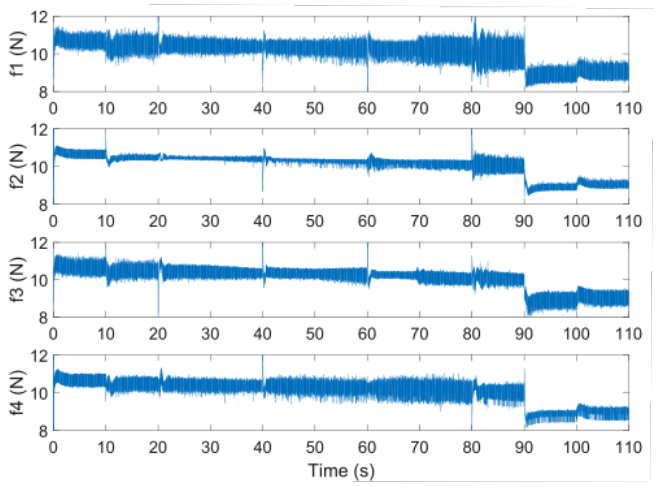

Fig. 7. Simulation results of control inputs.

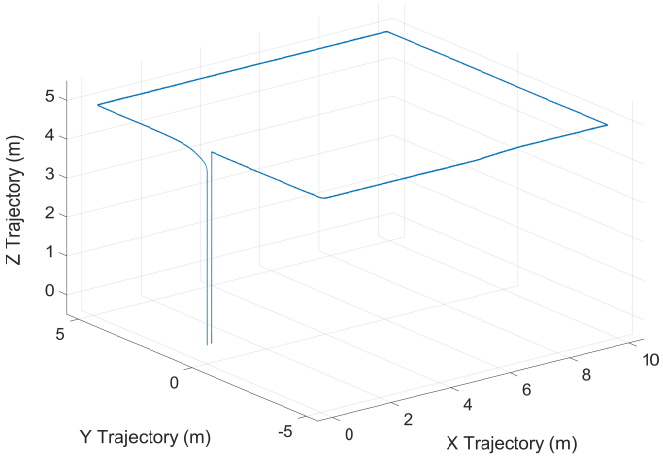

Fig. 8. 3D position tracking.

In summary, it is observed that there are errors in an average of 0.20 m for the transient and steady-state conditions as depicted in Fig. 5. The reasons can be, on one hand, due to the sub-optimal gains obtained heuristically, and, on the other hand, due to the choice of the sliding surface. Also, in Fig. 7, we can see that the chattering effect is in a range of 2 N and its high switching frequency is a known characteristic of the continuous sliding mode controller. Note that the obtained results can be improved by (i) adding an integral part in the sliding surface which also will increase the complexity for the determination of the gains, (ii) with better gain values using optimization algorithms. Nevertheless, by analyzing the tracking trajectory, the obtained results are satisfactory, taking into account the curve of the desired trajectory (Fig. 5 and Fig. 6) and the uncertainties.

VI. Conclusions

In this work, a cascade sliding mode controller was simulated with exponential reaching law in the outer control loop and Modified STA in the inner control loop, under noise conditions and unmodelled dynamics the controller performs well and can be improved by optimizing the controller's gains. This choice belongs to the fact that the inner control loop must be faster than the outer control loop. This condition is satisfied since the modified STA allows faster convergence and higher precision. The proposed combination has been tested on simulations where the results obtained showed good tracking performance even if the used model was highly uncertain.

Acknowledgements

The authors would like to thank to the Paraguayan Government for the financial support through CONACYT research project (PINV15-0136).

References

[1] Z. Yingkun, "Flight path planning of agriculture uav based on improved artificial potential field method," in *2018 Chinese Control And Decision Conference (CCDC)*, June 2018, pp. 1526–1530.

[2] M. Gomez-Redondo, H. Fretes, J. Rodríguez-Piñeiro, J. Rodas, and R. Gregor, "Automatic scene reconstruction algorithm for planialtimetric applications," in *2018 IEEE International Conference on Automation/XXIII Congress of the Chilean Association of Automatic Control (ICA-ACCA)*, Oct 2018, pp. 1–6.

[3] V. N. Nguyen, R. Jenssen, and D. Roverso, "Intelligent monitoring and inspection of power line components powered by uavs and deep learning," *IEEE Power and Energy Technology Systems Journal*, vol. 6, no. 1, pp. 11–21, March 2019.

[4] A. Altan, O. Aslan, and R. Hacıoğlu, "Real-time control based on narx neural network of hexarotor uav with load transporting system for path tracking," in *2018 6th International Conference on Control Engineering Information Technology (CEIT)*, Oct 2018, pp. 1–6.

[5] Z. Liu, X. Liu, J. Chen, and C. Fang, "Altitude control for variable load quadrotor via learning rate based robust sliding mode controller," *IEEE Access*, vol. 7, pp. 9736–9744, 2019.

[6] Z. Xu, H. Shi, N. Li, C. Xiang, and H. Zhou, "Vehicle detection under uav based on optimal dense yolo method," in *2018 5th International Conference on Systems and Informatics (ICSAI)*, Nov 2018, pp. 407–411.

[7] H. Shakhatreh, A. H. Sawalmeh, A. Al-Fuqaha, Z. Dou, E. Almaita, I. Khalil, N. S. Othman, A. Khreishah, and M. Guizani, "Unmanned aerial vehicles (uavs): A survey on civil applications and key research challenges," *IEEE Access*, vol. 7, pp. 48 572–48 634, 2019.

[8] C. Liu, J. Pan, and Y. Chang, "Pid and lqr trajectory tracking control for an unmanned quadrotor helicopter: Experimental studies," in *2016 35th Chinese Control Conference (CCC)*, July 2016, pp. 10 845–10 850.

[9] V. Utkin, J. Guldner, and J. Shi, *Sliding mode control in electromechanical systems*. Taylor-Francis, 1999.

[10] Y. Kali, J. Rodas, M. Ayala, M. Saad, R. Gregor, K. Benjelloun, J. Doval-Gandoy, and G. Goodwin, "Discrete-time sliding mode with time delay estimation of a six-phase induction motor drive," in *IECON 2018 - 44th Annual Conference of the IEEE Industrial Electronics Society*, Oct 2018, pp. 5807–5812.

[11] Y. Kali, M. Ayala, J. Rodas, M. Saad, J. Doval-Gandoy, R. Gregor, and K. Benjelloun, "Current control of a six-phase induction machine drive based on discrete-time sliding mode with time delay estimation," *Energies*, vol. 12, no. 1, 2019.

[12] Y. Feng, X. Yu, and Z. Man, "Non-singular terminal sliding mode control of rigid manipulators," *Automatica*, vol. 38, no. 12, pp. 2159 – 2167, 2002.

[13] Y. Kali, M. Saad, K. Benjelloun, and M. Benbrahim, "Sliding mode with time delay control for mimo nonlinear systems with unknown dynamics," in *2015 International Workshop on Recent Advances in Sliding Modes (RASM)*, April 2015, pp. 1–6.

[14] K. Runcharoon and V. Srichatrapimuk, "Sliding mode control of quadrotor," in *TAEECE, International Conference on Technological Advances in Electrical, Electronics and Computer Engineering*, May 2013, pp. 552–557.

[15] I. Boiko and L. Fridman, "Analysis of chattering in continuous sliding-mode controllers," *IEEE Transactions on Automatic Control*, vol. 50, no. 9, pp. 1442–1446, Sept 2005.

[16] M. Tseng and M. Chen, "Chattering reduction of sliding mode control by low-pass filtering the control signal," *Asian Journal of Control*, vol. 12, no. 3, pp. 392–398, 2010.

[17] D. Lee, H. Jin Kim, and S. Sastry, "Feedback linearization vs. adaptive sliding mode control for a quadrotor helicopter," *International Journal of Control, Automation and Systems*, vol. 7, no. 3, pp. 419–428, Jun 2009.

[18] Y. Kali, J. Rodas, R. Gregor, M. Saad, and K. Benjelloun, "Attitude tracking of a tri-rotor uav based on robust sliding mode with time delay estimation," in *2018 International Conference on Unmanned Aircraft Systems (ICUAS)*, June 2018, pp. 346–351.

[19] L. Besnard, Y. B. Shtessel, and B. Landrum, "Quadrotor vehicle control via sliding mode controller driven by sliding mode disturbance observer," *Journal of the Franklin Institute*, vol. 349, no. 2, pp. 658 – 684, 2012.

[20] A. Levant, "Higher-order sliding modes, differentiation and output-feedback control," *International Journal of Control*, vol. 76, no. 9-10, pp. 924–941, 2003.

[21] Y. Kali, M. Saad, and K. Benjelloun, "Non-singular terminal second order sliding mode with time delay estimation for uncertain robot manipulators," in *ICINCO, International Conference on Informatics in Control, Automation and Robotics*, 2017, pp. 226–232.

[22] Y. Kali, M. Saad, K. Benjelloun, and A. Fatemi, "Discrete-time second order sliding mode with time delay control for uncertain robot manipulators," *Robotics and Autonomous Systems*, vol. 94, pp. 53 – 60, 2017.

[23] A. Benallegue, A. Mokhtari, and L. Fridman, "High-order sliding-mode observer for a quadrotor UAV," *International Journal of Robust and Nonlinear Control*, vol. 18, no. 4-5, pp. 427–440, 2008.

[24] I. González-Hernández, S. Salazar, F. Munoz, and R. Lozano, "Super-twisting control scheme for a miniature quadrotor aircraft: Application to trajectory-tracking problem," in *ICUAS, International Conference on Unmanned Aircraft Systems*, June 2017, pp. 1547–1554.

[25] I. González-Hernández, F. M. Palacios, S. S. Cruz, E. S. E. Quesada, and R. L. Leal, "Real-time altitude control for a quadrotor helicopter using a super-twisting controller based on high-order sliding mode observer," *International Journal of Advanced Robotic Systems*, vol. 14, no. 1, pp. 1–15, 2017.

[26] E. Ibarra and P. Castillo, "Nonlinear super twisting algorithm for UAV attitude stabilization," in *ICUAS, International Conference on Unmanned Aircraft Systems*, June 2017, pp. 640–645.

[27] Y. Kali, M. Saad, K. Benjelloun, and C. Khairallah, "Super-twisting algorithm with time delay estimation for uncertain robot manipulators," *Nonlinear Dynamics*, vol. 93, no. 2, pp. 557–569, Jul 2018.

[28] E. Paiva, J. Rodas, Y. Kali, R. Gregor, and M. Saad, "Robust flight control of a tri-rotor uav based on modified super-twisting algorithm," in *2019 International Conference on Unmanned Aircraft Systems (ICUAS)*, June 2019, pp. 551–556.

[29] R. W. Beard and T. W. McLain, *Small Unmanned Aircraft: Theory and Practice*. Princeton, NJ, USA: Princeton University Press, 2012.

[30] C. J. Fallaha, M. Saad, H. Y. Kanaan, and K. Al-Haddad, "Sliding-mode robot control with exponential reaching law," *IEEE Transactions on Industrial Electronics*, vol. 58, no. 2, pp. 600–610, Feb 2011.

[31] Y. Kali, M. Saad, and K. Benjelloun, *Control of Robot Manipulators Using Modified Backstepping Sliding Mode*. Singapore: Springer Singapore, 2019, pp. 107–136.

[32] Y. Kali, K. Benjelloun, M. Saad, and M. Benbrahim, "Non-singular terminal sliding mode with time delay control for uncertain 2nd order nonlinear systems," in *2017 14th International Multi-Conference on Systems, Signals Devices (SSD)*, March 2017, pp. 625–630.